

# Tweezers controlled resonator

Samuel Kaminski,<sup>1</sup> Leopoldo L. Martin,<sup>1</sup> and Tal Carmon<sup>1</sup>

<sup>1</sup>*Technion- Israel Institute of Technology, 3200003 Haifa, Israel*  
*\*tcarmon@technion.ac.il*

**Abstract:** We experimentally demonstrate trapping a microdroplet by using an optical tweezer and then activating it as a microresonator by bringing it close to a tapered-fiber coupler. Our tweezers facilitated the tuning of the coupling from the under-coupled to the critically-coupled regime while the quality-factor [Q] is 12 million and the resonator's size is at the 80  $\mu\text{m}$  scale.

©2015 Optical Society of America

**OCIS codes:** (140.7010) Laser trapping; (140.4780) Optical resonators; (140.3945) Microcavities.

---

## References and links

1. S. C. Kuo and M. P. Sheetz, "Force of single kinesin molecules measured with optical tweezers," *Science* **260**(5105), 232–234 (1993).
2. S. M. Block, L. S. Goldstein, and B. J. Schnapp, "Bead movement by single kinesin molecules studied with optical tweezers," *Nature* **348**(6299), 348–352 (1990).
3. K. C. Neuman and A. Nagy, "Single-molecule force spectroscopy: optical tweezers, magnetic tweezers and atomic force microscopy," *Nat. Methods* **5**(6), 491–505 (2008).
4. D. G. Grier, "A revolution in optical manipulation," *Nature* **424**(6950), 810–816 (2003).
5. J. E. Curtis, B. A. Koss, and D. G. Grier, "Dynamic holographic optical tweezers," *Opt. Commun.* **207**(1-6), 169–175 (2002).
6. A. Terray, J. Oakey, and D. W. Marr, "Fabrication of linear colloidal structures for microfluidic applications," *Appl. Phys. Lett.* **81**(9), 1555–1557 (2002).
7. L. Paterson, M. P. MacDonald, J. Arlt, W. Sibbett, P. E. Bryant, and K. Dholakia, "Controlled rotation of optically trapped microscopic particles," *Science* **292**(5518), 912–914 (2001).
8. M. Reicherter, T. Haist, E. U. Wagemann, and H. J. Tiziani, "Optical particle trapping with computer-generated holograms written on a liquid-crystal display," *Opt. Lett.* **24**(9), 608–610 (1999).
9. J. P. Pantina and E. M. Furst, "Directed assembly and rupture mechanics of colloidal aggregates," *Langmuir* **20**(10), 3940–3946 (2004).
10. A. D. Ward, M. G. Berry, C. D. Mellor, and C. D. Baine, "Optical sculpture: controlled deformation of emulsion droplets with ultralow interfacial tensions using optical tweezers," *Chem. Commun. (Camb.)* **2006**(43), 4515–4517 (2006).
11. A. Terray, J. Oakey, and D. W. Marr, "Microfluidic control using colloidal devices," *Science* **296**(5574), 1841–1844 (2002).
12. A. Ashkin and J. Dziedzic, "Observation of resonances in the radiation pressure on dielectric spheres," *Phys. Rev. Lett.* **38**(23), 1351–1354 (1977).
13. H.-M. Tzeng, K. F. Wall, M. B. Long, and R. K. Chang, "Laser emission from individual droplets at wavelengths corresponding to morphology-dependent resonances," *Opt. Lett.* **9**(11), 499–501 (1984).
14. M. Hossein-Zadeh and K. J. Vahala, "Fiber-taper coupling to Whispering-Gallery modes of fluidic resonators embedded in a liquid medium," *Opt. Express* **14**(22), 10800–10810 (2006).
15. A. Jonáš, Y. Karadag, M. Mestre, and A. Kiraz, "Probing of ultrahigh optical Q-factors of individual liquid microdroplets on superhydrophobic surfaces using tapered optical fiber waveguides," *J. Opt. Soc. Am. B* **29**(12), 3240–3247 (2012).
16. U. Levy, K. Campbell, A. Groisman, S. Mookherjee, and Y. Fainman, "On-chip microfluidic tuning of an optical microring resonator," *Appl. Phys. Lett.* **88**(11), 111107 (2006).
17. J. C. Knight, G. Cheung, F. Jacques, and T. A. Birks, "Phase-matched excitation of whispering-gallery-mode resonances by a fiber taper," *Opt. Lett.* **22**(15), 1129–1131 (1997).
18. M. Cai, O. Painter, and K. J. Vahala, "Observation of critical coupling in a fiber taper to a silica-microsphere whispering-gallery mode system," *Phys. Rev. Lett.* **85**(1), 74–77 (2000).
19. S. M. Spillane, T. J. Kippenberg, O. J. Painter, and K. J. Vahala, "Ideality in a fiber-taper-coupled microresonator system for application to cavity quantum electrodynamics," *Phys. Rev. Lett.* **91**(4), 043902 (2003).
20. T. Carmon, L. Yang, and K. Vahala, "Dynamical thermal behavior and thermal self-stability of microcavities," *Opt. Express* **12**(20), 4742–4750 (2004).
21. T. J. Kippenberg, S. M. Spillane, and K. J. Vahala, "Kerr-nonlinearity optical parametric oscillation in an ultrahigh-Q toroid microcavity," *Phys. Rev. Lett.* **93**(8), 083904 (2004).

22. T. Carmon and K. J. Vahala, "Visible continuous emission from a silica microphotonic device by third-harmonic generation," *Nat. Phys.* **3**(6), 430–435 (2007).
23. I. S. Grudin, A. B. Matsko, and L. Maleki, "Brillouin lasing with a CaF<sub>2</sub> whispering gallery mode resonator," *Phys. Rev. Lett.* **102**(4), 043902 (2009).
24. M. Tomes and T. Carmon, "Photonic micro-electromechanical systems vibrating at X-band (11-GHz) rates," *Phys. Rev. Lett.* **102**(11), 113601 (2009).
25. G. Bahl, J. Zehnpfennig, M. Tomes, and T. Carmon, "Stimulated optomechanical excitation of surface acoustic waves in a microdevice," *Nat. Commun.* **2**, 403 (2011).
26. A. B. Matsko, A. A. Savchenkov, V. S. Ilchenko, D. Seidel, and L. Maleki, "Optomechanics with surface-acoustic-wave whispering-gallery modes," *Phys. Rev. Lett.* **103**(25), 257403 (2009).
27. P. R. Cooper, "Refractive-index measurements of paraffin, a silicone elastomer, and an epoxy resin over the 500–1500-nm spectral range," *Appl. Opt.* **21**(19), 3413–3415 (1982).
28. M. L. Gorodetsky and V. S. Ilchenko, "Optical microsphere resonators: optimal coupling to high-Q whispering-gallery modes," *J. Opt. Soc. Am. B* **16**(1), 147–154 (1999).
29. B. Min, L. Yang, and K. Vahala, "Controlled transition between parametric and Raman oscillations in ultrahigh-Q silica toroidal microcavities," *Appl. Phys. Lett.* **87**(18), 181109 (2005).
30. G. Bahl, K. H. Kim, W. Lee, J. Liu, X. Fan, and T. Carmon, "Brillouin cavity optomechanics with microfluidic devices," *Nat. Commun.* **4**, 1994 (2013).
31. F. Vollmer and S. Arnold, "Whispering-gallery-mode biosensing: label-free detection down to single molecules," *Nat. Methods* **5**(7), 591–596 (2008).

## 1. Introduction

Optical traps serve in the most sensitive biological-force measurements [1–3] as well as in chemistry and physics research [4]. As optical tweezers can trap almost perfectly spherical droplets while precisely controlling their position, it is natural to check if we can activate tweezed droplets as optical microresonators. By doing so, one can benefit from modern tweezing techniques such as dynamical holograms [5] that can simultaneously manipulate multiple particles [6–9]. Further, traps were shown to sculpt microdroplets into elliptical, triangular and rectangular shapes [10] which can serve in deforming the resonator while light is inside. Additionally pumps and valves [11] were shaped by trapping several adjacent spheres. Such adjacent spheres [11] can serve as cascaded resonators that one can shape each of them [10] as desired and then position in the place where they are needed [11]. Interestingly, one of the first experiments in microcavities was done using an optically trapped droplet resonator [12]. In this experiment, Ashkin was tuning the frequency of a laser beam that was trapping a microdrop against gravity. An upward motion of the drop indicated that the laser frequency was near resonance.

Our long-term vision includes optical circuits where a multi-minima optical trap shapes and positions multiple optical components. Being practical and in order to start here with proving this concept, we use an optical trap to position a droplet next to a tapered fiber; and by this, activating the droplet as an optical resonator.

## 2. Experimental setup

As one can see in Fig. 1(a), our experimental setup consists of optical tweezers (green) that drag a droplet of high index material (yellow) and control its distance from a nearby tapered fiber (gray). Our setup is different from the current state of the art in nanopositioning of optical devices, which uses expensive and cumbersome positioners with an inch-scale footprint. Such nanopositioners are non-scalable to control multiple microresonators. On the contrary, optical tweezers were shown to control many devices with a single beam of light that is controlled by a spatial light modulator (SLM).

In the past, droplets were used as optical resonators [12–16], including while optically trapped [12]. Differently here, we optically trap our oil droplet in an aquatic environment next to a tapered-fiber coupler [17–19]. As will be explained in what follows, the optical tweezers enable controlling the distance between the resonator and the tapered fiber and therefore allows tuning the optical coupling upon need.

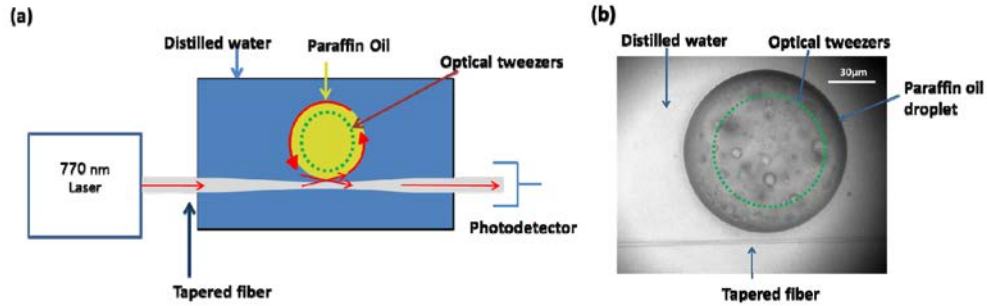


Fig. 1. **Experimental setup** (A) where light is coupled from a tapered fiber to circumferentially circulate into a microdroplet resonator. (B) A micrograph of our experiment. The dashed green circle represents the location of the optical tweezers that hold the droplet. The focuses in the micrograph were optimized separately (for the taper and for the drop).

The optical whispering gallery mode resonators are made by blending together in an ultrasonic bath for half an hour, paraffin oil (0.2 ml), distilled water (DI) (1 ml) and an emulsifier (0.1 ml of “Tween 40”). An aliquot form of the emulsion was mixed with DI water and injected into a 125  $\mu\text{m}$  deep flow cell. This flow cell contains a single-mode tapered fiber [17–19] which is placed in a water medium. The fiber’s diameter at the waste is small enough that the speed of light in the fiber is almost equal to the speed of light in the resonator. For this reason the tapered fiber is phase matched with the resonator which enables efficient coupling of light into the microdrop resonator. A laser source with an emission wavelength of 532 nm is focused downward using a GRIN lens (N.A. = 0.46,  $f = 2$  mm) and captures a single droplet in the flow cell. Simultaneously, a microscope is used to view the flow cell from below (Fig. 1(b)). The effective trapping power ranges from 5 to 20 mW using a typical working distance of 7 mm. The gradient force that the optical trap applies in the horizontal direction (i.e. transverse to beam propagation) serves in dragging the drop to a desired position. In this way, we trap a drop and move it towards the tapered fiber until achieving evanescent coupling [17–19] to the droplet [14, 15].

### 3. Experimental results

We experimentally monitor the optical transmission through the resonator by measuring the output power of our system (Fig. 1(a)). As expected, scanning our laser wavelength through resonance reveals a Lorentzian dip in the resonator’s transmission (Fig. 2). The linewidth of such resonances is inversely proportional to the resonator’s optical quality factor ( $Q$ ). Using this inverse relation between quality factor and linewidth we get an optical quality-factor of 12 million for our resonator. To ensure the validity of this result we eliminate linewidth broadening such as thermal broadening [20], by operating at the undercoupled regime and at low input-power levels. Another indication for the optical excitation of the resonances is revealed via residual scattering from imperfections near the cavity mode. While the laser is at the resonance wavelength, these scatterings in the surface of the oil drop are seen shining as shown in Fig. 2(c). We repeated this experiment several times using droplets between 70 to 120 microns in diameter, all resulting in similar resonances with similar quality factors.

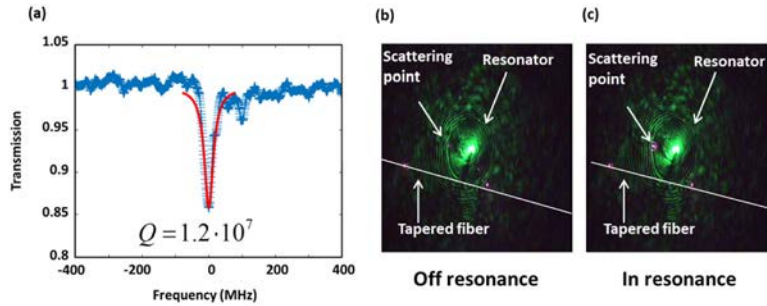


Fig. 2. **Experimental results: The optical quality factor,  $Q$ ,** is experimentally measured by (a) trapping a microsphere and bringing it near the evanescent field of the tapered fiber. When in the undercoupled regime, a Lorentzian drop in transmission is monitored with a linewidth that reveals a 12-million  $Q$ . While at resonance, the mode is seen via residual scatterings (c) that are not seen while off resonance (b).

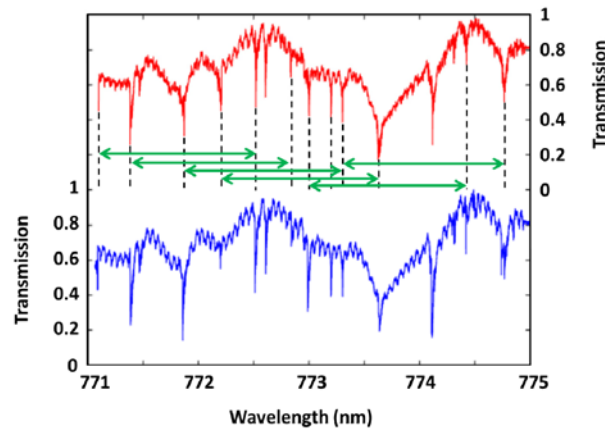


Fig. 3. **Experimental results: resonances spectrum** with several modes. To check that these modes are repeatable, we scan while increasing wavelength (red) and then while decreasing wavelength (blue) and verify that resonances indeed stay. The green arrows indicates the free spectral range.

We will now present a broader wavelength-scan experiment that reveals several resonances. In Fig. 3, we can see a 4 nm wavelength scan that reveals, as expected with such a spherical resonator, approximately 16 optical resonances. To confirm that these resonances are repeatable, we perform the scan twice. First, we scan to the longer wavelengths (Fig. 3 in red) and then to the shorter ones (Fig. 3 in blue). As expected, these two scans (Fig. 3 blue and red) produce an overlapping resonance spectra. A dense spectrum, as demonstrated in Fig. 3, can serve in the future for phase matching, as required for a variety of nonlinear effects including four waves mixing [21], third-harmonic generation [22], as well as backward [23, 24] and forward [25, 26] Brillouin scattering. An interesting detail of the spectra shown in Fig. 3 is that many of the peaks have a “sibling” located 1.43 nm away (green arrows). Accordingly in this regard, each of the cavity modes is expected to have an adjacent mode for which the number of optical waves along circumference is different by 1. The distance between these adjacent modes is generally referred to as the free spectral range,

$$FSR = \frac{\lambda^2}{2\pi R \cdot n_{eff}}, \quad (1)$$

where  $\lambda$  is the vacuum wavelength,  $R$  is the resonator radius and  $n_{eff}$  is the effective refractive index of the mode [27]. The radius measured by the microscope is:  $43 \pm 1 \mu\text{m}$ . Using Eq. (1)

with the measured radius and free spectral range (Fig. 3.), we obtain that our resonator has an effective refractive index of  $1.47 \pm 0.01$ .

We will now control the distance between the tapered-fiber and the resonator. We do so by changing the coupling distance between the fiber waveguide and the resonator. We start this experiment when the resonator is relatively far from the taper so that only 12% of the laser light is coupled into the resonator, as evident from the fact that transmission at resonance drops to 88% (Fig. 4(a)). This regime is generally referred to as the undercoupled regime [28]. We now move the resonator (by moving the optical tweezers) about 250 nm closer to the taper. As the resonator approaches the taper, the coupling increases until 93% of the light enters the resonator (Fig. 4(b)). Such a high absorption in the resonator indicates that the system is operating near the critically coupled regime [19, 28]. While at critical coupling, coupler loss is equal to the resonator loss, and most of the input power can be coupled into the resonator [28]. In this case, transmission may decrease to almost zero [19]. As we demonstrated (Fig. 4(a)-4(b)) in our experiment, the tweezers, enables control of the optical coupling from the under-coupled to the critically coupled regime. Controlling the coupling, as we perform here, was experimentally demonstrated in the past to be useful in reducing lasing threshold for Raman [29] and Brillouin [30] microlasers as well as for enabling selection between laser processes and parametric oscillations [29]. Additionally and as mentioned above, being able to tune coupling to the undercoupled regime implies a narrow resonance line that is less affected by thermal broadening [20] and therefore useful for sensing applications [31].

Interestingly, beyond a certain point the optical trap cannot push the drop any closer to the taper. This is because interfacial tension between the taper and water is large when compared to taper and oil. A small gap between the taper and the resonator is therefore always kept. If interfacial tension was not as is, then our experiment could end by a catastrophic collapse of the droplet towards coating the taper. Hence, repulsion between drop and taper is benefiting the durability of our resonator.

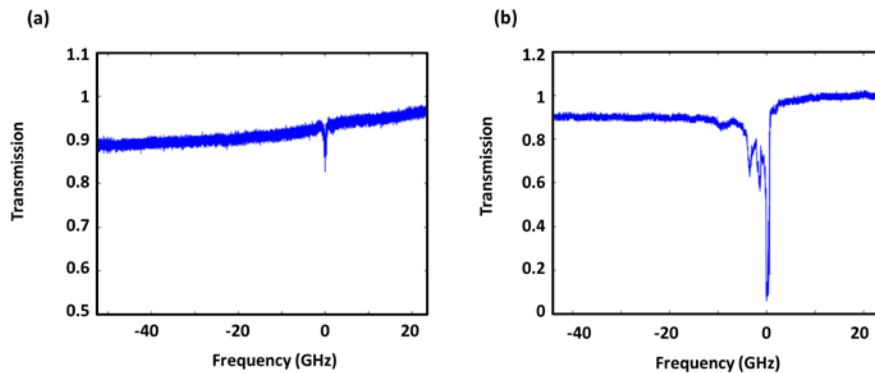


Fig. 4. **Experimental results, tunable coupling** from the undercoupled regime (a) to the critically coupled regime (b). During this measurement, the resonator is first trapped relatively far from the taper (a) and then brought closer to it (b).

#### 4. Conclusions

In conclusion, we prove the concept of using an optical trap for activating oil droplets as fiber-coupled microresonators. We believe that our technique will soon extend to several coupled resonators and then to an optical circuit where the shape and position of many optical devices will be controlled with light. Our technique might enable add-ons when compared to lithography of optical circuits. This is because the tweezers can move the optical devices while they are optically active (as we demonstrate in Fig. 4). Then, when such an optical inspection will reveal that the optical circuit is properly functioning, curing techniques will be used to turn the liquid circuit into a durable solid one.

Though many challenges are still on our way, optical traps can wave major technology stoppers in manipulating and changing the shape of multiple optical devices while precisely controlling their position.

### **Acknowledgments**

We acknowledge help from Ariel Bar Yehuda, Moran Bercovici, Carmel Rotschild and Eyal Zussman. This research was supported by ICore: the Israeli Excellence center “Circle of Light” and by the Israeli Science Foundation grant no. 2013/15.